Supplemental Document

Optics EXPRESS

Differentiable scattering matrix for optimization of photonic structures: supplement

ZIWEI ZHU AND CHANGXI ZHENG*

Department of Computer Science, Columbia University, New York, New York 10027, USA
*cxz@cs.columbia.edu

Supplement DOI: https://doi.org/10.6084/m9.figshare.13283540

Parent Article DOI: https://doi.org/10.1364/OE.409261

Differentiable Scattering Matrix for Optimization of Photonic Structures: supplemental document

This document provides supplementary information to the paper "Differentiable Scattering Matrix for Optimization of Photonic Structures".

1. MATRIX CONSTRUCTION IN RCWA

A. Construct Wave Equation Coefficient Matrices

When analyzing a meta-atom structure, we use z-direction to indicate the wave propagation direction, and use periodic boundary condition on x-y plane. In the framework of RCWA, the electric and magnetic fields at a distance z are represented under a set of Fourier basis functions (also called harmonics).

Suppose the E- and H-fields are both represented using $n_x \times n_y$ harmonics. The i-th harmonic along the x-axis together with the j-th harmonic along the y-axis describes a wave vector projected on the x-y plane, that is,

$$\begin{aligned}\vec{k}_{i,j} &= (k_{ix}, k_{jy}) \\ &= \left(\frac{2\pi}{L_x}\left(i - \frac{n_x+1}{2}\right), \frac{2\pi}{L_y}\left(j - \frac{n_y+1}{2}\right)\right)\end{aligned} \tag{S1}$$

where L_x and L_y are periods along x- and y-axis, respectively. When $i = \frac{n_x+1}{2}$ and $j = \frac{n_y+1}{2}$, the wave vector $\vec{k}_{i,j} = \vec{0}$, corresponding to the wave propagating only along z-direction.

With these Fourier basis functions, the E-field at a distance z can be expressed as

$$E(x,y,z) = \sum_{i=1}^{n_x}\sum_{j=1}^{n_y} c_{i,j}(z) e^{j(k_{ix}x + k_{jy}y)}, \tag{S2}$$

where $c_{i,j}(z)$ are Fourier coefficients, and they are functions of z. In other words, Eq. (S2) is a representation using separation of variables. It discretizes the field on x-y plane but remain analytic along z-direction. The H-field can be (semi-)discretized in the same way.

Substituting Eq. (S2) into the frequency-domain Maxwell's equations leads to the semi-discussed equations (2) in the main text. Here, for the sake of simplicity of the presentation and following the use in common situations, we assume the materials are non-ferromagnetic. Then, the coefficient matrices $\mathbf{P}$ and $\mathbf{Q}$ in Eqn. (2) have the following forms,

$$\begin{aligned}\mathbf{P} &= \begin{bmatrix} \mathbf{K}_x[[\epsilon]]^{-1}\mathbf{K}_y & k_0^2\mathbf{I} - \mathbf{K}_x[[\epsilon]]^{-1}\mathbf{K}_x \\ \mathbf{K}_y[[\epsilon]]^{-1}\mathbf{K}_y - k_0^2\mathbf{I} & -\mathbf{K}_y[[\epsilon]]^{-1}\mathbf{K}_x \end{bmatrix} \text{ and} \\ \mathbf{Q} &= \begin{bmatrix} -\mathbf{K}_x\mathbf{K}_y & \mathbf{K}_x\mathbf{K}_x - k_0^2[[\epsilon]] \\ k_0^2[[\epsilon]] - \mathbf{K}_y\mathbf{K}_y & \mathbf{K}_y\mathbf{K}_x \end{bmatrix},\end{aligned} \tag{S3}$$

where $k_0 = 2\frac{\pi}{\lambda}$ is the considered wavelength λ, $[[\epsilon]]$ is the matrix describing the permittivity distribution on x-y plane; its construction will be presented in the next subsection. Lastly, $\mathbf{K}_x$ and $\mathbf{K}_y$ are both diagonal matrices of size $n_x n_y \times n_x n_y$ [1], and the $\left[j-1+(i-1)n_y\right]$-th diagonal elements in $\mathbf{K}_x$ and $\mathbf{K}_y$ are expressed, respectively, as follows:

$$\begin{aligned}\mathbf{K}_x\left(j-1+(i-1)n_y\right) &= \frac{2}{L_x}\pi\left(i - \frac{n_x+1}{2}\right) \text{ and} \\ \mathbf{K}_y\left(j-1+(i-1)n_y\right) &= \frac{2}{L_y}\pi\left(j - \frac{n_y+1}{2}\right).\end{aligned} \tag{S4}$$

In the expressions of $\mathbf{P}$ and $\mathbf{Q}$, k_0, $\mathbf{K}_x$, and $\mathbf{K}_y$ are all independent from the structural design parameters; they are constant values when one take the derivatives with respect to design

parameters. The permittivity matrix $[[\epsilon]]$, however, will change with respect to the design parameters. Therefore, the derivatives of the coefficient matrices have the forms,

$$\begin{aligned} \mathrm{d}\mathbf{P} &= \begin{bmatrix} \mathbf{K}_x \mathrm{d}[[\epsilon]]^{-1}\mathbf{K}_y & -\mathbf{K}_x \mathrm{d}[[\epsilon]]^{-1}\mathbf{K}_x \\ \mathbf{K}_y \mathrm{d}[[\epsilon]]^{-1}\mathbf{K}_y & -\mathbf{K}_y \mathrm{d}[[\epsilon]]^{-1}\mathbf{K}_x \end{bmatrix} \text{ and} \\ \mathrm{d}\mathbf{Q} &= \begin{bmatrix} \mathbf{0} & -k_0^2 \mathrm{d}[[\epsilon]] \\ k_0^2 \mathrm{d}[[\epsilon]] & \mathbf{0} \end{bmatrix} \end{aligned} \tag{S5}$$

where the symbol d indicates the derivative with respect to a particular design parameter p, and $\mathrm{d}[[\epsilon]]^{-1}$ can be expressed as

$$\mathrm{d}[[\epsilon]]^{-1} = -[[\epsilon]]^{-1}\mathrm{d}[[\epsilon]][[\epsilon]]^{-1}. \tag{S6}$$

Discussion. Closely related to RCWA is another semi-analytical method, the method of line. In the method of line, the only difference from RCWA is that the E- and H-fields on the x-y plane are represented in a discretized spatial domain, unlike RCWA's representation in the Fourier domain (i.e., using Eqs. (S1) and (S2)). This leads to different matrices $\mathbf{P}$ and $\mathbf{Q}$ and their derivatives $\mathrm{d}\mathbf{P}$ and $\mathrm{d}\mathbf{Q}$. But the rest of the computation (including the derivative computation presented in this paper) stays the same. In this paper, we demonstrate the derivative computation in RCWA.

B. Permittivity Matrix of Grid-discretized Shapes

To construct the permittivity matrix $[[\epsilon]]$ in Eq. (S3), we consider the cross-sectional region of the photonic structure on x-y plane. Suppose the region has a size $L_x \times L_y$. The continuous Fourier transform of the permittivity distribution in this region is written as

$$\epsilon(m,n) = \frac{1}{S}\int\int_{\mathcal{S}} \epsilon(x,y) e^{\left(-i\frac{2\pi}{L_x}mx\right)} e^{\left(-i\frac{2\pi}{L_y}ny\right)} \mathrm{d}x\mathrm{d}y \tag{S7}$$

where $\mathcal{S}$ is the cross-sectional region and S is its area.

To compute Eq. (S7) numerically, we first divide the cross-sectional region into $P_x \times P_y$ grids. Assume that the permittivity in each grid (l,p) is uniformly distributed, denoted as $\epsilon_{l,p}$. Then, the (discrete) Fourier transform of all grids is a summation of the Fourier transform of each grid, namely,

$$\begin{aligned} \epsilon(m,n) = \sum_{l=1}^{P_x}\sum_{p=1}^{P_y} \epsilon_{l,p} &\left[\frac{1}{L_x}\exp\left(-i\frac{m\pi}{L_x}\left(u_l+u_{l-1}\right)\right)\ \mathrm{sinc}\left(\frac{m\pi}{L_x}\left(u_l-u_{l-1}\right)\right)\left(u_l-u_{l-1}\right)\right] \\ &\times\left[\frac{1}{L_y}\exp\left(-i\frac{n\pi}{L_y}\left(v_p+v_{p-1}\right)\right)\ \mathrm{sinc}\left(\frac{n\pi}{L_y}\left(v_p-v_{p-1}\right)\right)\left(v_p-v_{p-1}\right)\right], \end{aligned} \tag{S8}$$

where $\mathrm{sinc}(x) = \frac{\sin x}{x}$, u_l is the x-coordinate of the l-th vertical grid line, and v_p is the y-coordinate of the p-th horizontal grid line. m and n are indices of the discrete Fourier coefficients: $m = -(n_x-1), \cdots, 0, 1, \cdots, (n_x-1)$ and $n = -(n_y-1), \cdots, 0, 1, \cdots, (n_y-1)$.

After computing $\epsilon(m,n)$ for all m and n, we can construct the permittivity matrix $[[\epsilon]]$, which has the size $n_x n_y \times n_x n_y$. The matrix $[[\epsilon]]$ has the so-called block-Toeplitz structure, containing matrix blocks that are repeated down the diagonals of the matrix. Its element values are assembled from the Fourier coefficients $\epsilon(m,n)$ in the following way:

$$[[\epsilon]]\left(in_y+j, kn_y+l\right) = \epsilon\left(i-k, j-l\right), \tag{S9}$$

where the indices i and k are in the range $0,\ldots,n_x-1$; j and l are in the range $0,\ldots,n_y-1$.

Similarly, the derivative of $[[\epsilon]]$ with respect to a design parameter can be computed using

$$\mathrm{d}[[\epsilon]]\left(in_y+j, kn_y+l\right) = \mathrm{d}\epsilon\left(i-k, j-l\right), \tag{S10}$$

where the scalar derivative $\mathrm{d}\epsilon\left(i-k, j-l\right)$ is computed by differentiating Eq. (S8) with respect to the design parameter.

C. Permittivity Matrix of Star-Convex Shapes

For a star-convex shape discussed in Section 4.B (recall Fig. 8) of the main text, we do not need to discretize the shape into grid-based representation. Suppose the shape is described by the parameters $p_1, \ldots, p_N$ (recall Fig. 8-a in the main text). As derived in [2], in this case the Fourier transform (S7) can be computed directly:

$$\tilde{\epsilon}(m,n) = \frac{1}{S}\sum_{k=1}^{N} \underbrace{\exp\left(j\vec{w}\cdot\vec{p}_k\right)\frac{\hat{n}\times\vec{\alpha}_k\cdot\vec{\alpha}_{k-1}}{(\vec{w}\cdot\vec{\alpha}_k)(\vec{w}\cdot\vec{\alpha}_{k-1})}}_{E_k}, \tag{S11}$$

where $\hat{n} = (0,0,1)$ is the z-axis vector, $\vec{w} = \left(-2\pi\frac{m}{L_x}, -2\pi\frac{n}{L_y}\right)$, and $\vec{\alpha}_k = \vec{p}_{k+1} - \vec{p}_k$.

There exist two corner cases in which the denominator in Eq. (S11) vanishes, and thus they require special treatments:

1. When $m = n = 0$, the vector $\vec{w}$ in Eq. (S11) vanishes. In this case, we resort to the continuous Fourier transform Eq. (S7), which leads to $\tilde{\epsilon}(0,0) = 1$.

2. $\vec{w}$ may become perpendicular to $\vec{\alpha}_k$, and we have

$$\vec{w}\cdot\vec{\alpha}_k = 0 \text{ and } \vec{w}\cdot\vec{p}_{k+1} = \vec{w}\cdot\vec{p}_k. \tag{S12}$$

In this case, we consider two terms E_k and E_{k+1} in the summation (S11). It can be shown that $E_k + E_{k+1} = \frac{0}{0}$, which is mathematically undefined. Instead, $E_k + E_{k+1}$ should be defined as its limit as the parameter p_k (i.e., the length of $\vec{p}_k$) approaches to the situation where $\vec{w}\cdot\vec{\alpha}_k = 0$ occurs. This limit can be computed using L'Hôpital's rule, by taking the derivatives of both the numerator and the denominator with respect to p_k. This process leads to the following form:

$$\begin{aligned} E_k + E_{k+1} = \exp\left(j\vec{w}\cdot\vec{p}_k\right)\Bigg\{ &-\frac{[\hat{p}_k\cdot(\hat{n}\times(\vec{a}_k+\vec{a}_{k-1}))]}{(\vec{w}\cdot\hat{p}_k)(\vec{w}\cdot\vec{a}_{k-1})} + \frac{[(\hat{n}\times\vec{a}_{k+1})\cdot\hat{p}_k]}{(\vec{w}\cdot\hat{p}_k)(\vec{w}\cdot\vec{a}_{k+1})} \\ &- j\frac{[(\hat{n}\times\vec{a}_k)\cdot\vec{a}_{k-1}]}{(\vec{w}\cdot\vec{a}_{k-1})} - \frac{[(\hat{n}\times\vec{a}_{k+1})\cdot\vec{a}_k]}{(\vec{w}\cdot\vec{a}_{k-1})(\vec{w}\cdot\vec{a}_{k+1})}\Bigg\} \end{aligned} \tag{S13}$$

Here it is safe to assume that $\vec{w}$ is *not* perpendicular to $\vec{\alpha}_{k-1}$ or $\vec{\alpha}_{k+1}$. This is because, if it is indeed perpendicular to $\vec{\alpha}_{k-1}$, then $\vec{p}_{k-1}$, $\vec{p}_k$, and $\vec{p}_{k+1}$ are co-linear, and we can discard the parameter p_k while still representing the same star-convex shape. Similarly, if $\vec{w}$ is perpendicular to $\vec{\alpha}_{k+1}$, we can safely discard p_{k+1}.

Lastly, note that $\tilde{\epsilon}(m,n)$ in Eq. (S11) is merely the Fourier transform of the star-convex shape, but not the entire material in an $L_x \times L_y$ region. The permittivity distribution in the entire region can be viewed as a superposition of a background permittivity ϵ_0 and a star-convex shape with the permittivity $\epsilon_1 - \epsilon_0$. Thus the Fourier transform of the entire permittivity distribution is the Fourier transforms of both components:

$$\epsilon(m,n) = \begin{cases} \frac{\epsilon_1-\epsilon_0}{L_xL_y}\tilde{\epsilon}(m,n) + \epsilon_0, \text{ if } m = n = 0; \\ \frac{\epsilon_1-\epsilon_0}{L_xL_y}\tilde{\epsilon}(m,n), \text{ Otherwise.} \end{cases} \tag{S14}$$

Once $\epsilon(m,n)$ for all m and n are obtained, we can assemble the permittivity matrix $[[\epsilon]]$ and compute its derivative $\mathrm{d}[[\epsilon]]$ using the same formula (S9) and (S10) presented earlier.

2. AN EXAMPLE OF EIGENVECTOR DISCONTINUITY

Figure 2 in the main text provides an exemplar meta-atom structure in which repeated eigenvalues (and thus repeated propagation constants) exist. Here we use a simple mathematical example to show that when repeated eigenvalues emerge, the eigenvector derivatives become undefined.

Consider the following 2×2 matrix with a parameter p:

$$\mathbf{A}(p) = \begin{bmatrix} 1 & p \\ p & 1 \end{bmatrix}. \tag{S15}$$

When $p \neq 0$, its eigenvectors form a constant matrix.

$$\mathbf{X} = \begin{bmatrix} -\frac{\sqrt{2}}{2} & \frac{\sqrt{2}}{2} \\ \frac{\sqrt{2}}{2} & \frac{\sqrt{2}}{2} \end{bmatrix}. \tag{S16}$$

In fact, when $p \neq 0$, this eigenvector matrix is unique up to a scale. When p becomes zero, repeated eigenvalues emerge (both are 1). However, while $\mathbf{X}$ is still a valid eigenvector matrix of $\mathbf{A}(0)$, it is not unique anymore. In fact, any 2×2 orthonormal matrix is a valid eigenvector matrix of $\mathbf{A}(0)$. For example, the standard eigen-decomposition solver (e.g., in Matlab) gives

$$\mathbf{X}(0) = \begin{bmatrix} 1 & 0 \\ 0 & 1 \end{bmatrix}. \tag{S17}$$

Therefore, in the presence of repeated eigenvalues, the non-uniqueness of eigenvectors causes the eigenvector derivatives undefined—in this case, an infinitesimal deviation from $p = 0$, can cause the eigenvectors to change from Eq. (S17) to Eq. (S16), discontinuously.

Remark. In this simple example, the discontinuity can be fixed by examining the limit of the $\mathbf{X}$ derivative as p approaches 0, because in this case the derivative of $\mathbf{X}$ at $p \neq 0$ is well-defined. However, the situations encountered in many photonic design tasks can be much more challenging. For example, in Fig. 2 of the main text, not only are the eigenvalues (i.e., effective indices) repeated, their derivatives with respect to the parameter are also repeated (e.g, see mode 0 and mode 1 in Fig. 2-c). In those cases, the derivative of $\mathbf{X}$ is not well-defined any more. If up to the n-th order derivatives of the eigenvalues are repeated, one has to rely on the $n+1$-th order derivative of $\mathbf{X}$ to resolve the discontinuity. This is a rather expensive, if not impossible, computational process.

3. DERIVATION OF EQUATIONS (5)

Here we present the derivation of Eqs. (5) in the main text. Starting from Eqs. (3), we first rewrite them as

$$\begin{aligned} \mathbf{R}_{\mathrm{L}} = \mathbf{R}_{\mathrm{R}} &= \left[\mathbf{I} - \left(\mathbf{A}^{-1}\mathbf{X}\mathbf{B}\right)^2\right]^{-1} \mathbf{A}^{-1}\left(\mathbf{X}\mathbf{B}\mathbf{A}^{-1}\mathbf{X}\mathbf{A} - \mathbf{B}\right) \\ &= \left[\mathbf{I} - \left(\mathbf{A}^{-1}\mathbf{X}\mathbf{B}\right)^2\right]^{-1} \left(\mathbf{A}^{-1}\mathbf{X}\mathbf{B}\mathbf{A}^{-1}\mathbf{X}\mathbf{A} - \mathbf{A}^{-1}\mathbf{B}\right) \\ &= \left(\mathbf{I} - \mathbf{D}_1^2\right)^{-1} \left(\mathbf{D}_1\mathbf{D}_2 - \mathbf{D}_3\right), \end{aligned} \tag{S18}$$

and

$$\begin{aligned} \mathbf{T}_{\mathrm{LR}} = \mathbf{T}_{\mathrm{RL}} &= \left(\mathbf{A} - \mathbf{X}\mathbf{B}\mathbf{A}^{-1}\mathbf{X}\mathbf{B}\right)^{-1} \mathbf{X}\left(\mathbf{A} - \mathbf{B}\mathbf{A}^{-1}\mathbf{B}\right) \\ &= \left[\mathbf{I} - \left(\mathbf{A}^{-1}\mathbf{X}\mathbf{B}\right)^2\right]^{-1} \mathbf{A}^{-1}\mathbf{X}\mathbf{A}\left[\mathbf{I} - (\mathbf{A}^{-1}\mathbf{B})^2\right] \\ &= \left[\mathbf{I} - \left(\mathbf{A}^{-1}\mathbf{X}\mathbf{B}\right)^2\right]^{-1} \left(\mathbf{A}^{-1}\mathbf{X}\mathbf{A} - \mathbf{A}^{-1}\mathbf{X}\mathbf{B}\mathbf{A}^{-1}\mathbf{B}\right) \\ &= \left(\mathbf{I} - \mathbf{D}_1^2\right)^{-1} \left(\mathbf{D}_2 - \mathbf{D}_1\mathbf{D}_3\right). \end{aligned} \tag{S19}$$

In the above two expressions, the three matrix notations are defined as

$$\mathbf{D}_1 \coloneqq \mathbf{A}^{-1}\mathbf{X}\mathbf{B},\ \mathbf{D}_2 \coloneqq \mathbf{A}^{-1}\mathbf{X}\mathbf{A},\ \text{and}\ \mathbf{D}_3 \coloneqq \mathbf{A}^{-1}\mathbf{B}. \tag{S20}$$

To reach the expressions in Eqs. (6) of the main text, we first rewrite the expressions of $\mathbf{A}$ and $\mathbf{B}$ in Eqs. (4) as the following forms:

$$\begin{aligned} \mathbf{A} &= \mathbf{W}^{-1}(\mathbf{W}_0 + \mathbf{W}\mathbf{V}^{-1}\mathbf{W}_0) \text{ and} \\ \mathbf{B} &= \mathbf{W}^{-1}(\mathbf{W}_0 - \mathbf{W}\mathbf{V}^{-1}\mathbf{W}_0). \end{aligned} \tag{S21}$$

Notice that $\mathbf{T}$, defined as $\mathbf{T} := \mathbf{\Omega Q}^{-1}$ in Sec. 3.B of the main text, has the equality relation $\mathbf{T} = \mathbf{W V}^{-1}$. This is because, as introduced in Sec. 2, $\mathbf{V}$ is related to $\mathbf{W}$ through $\mathbf{V} = \mathbf{QW\Lambda}^{-1}$, and thus we have

$$\mathbf{V} = \mathbf{QW\Lambda}^{-1} = \mathbf{Q\Omega}^{-1}\mathbf{\Omega W\Lambda}^{-1} = \mathbf{Q\Omega}^{-1}\mathbf{W} = \mathbf{T}^{-1}\mathbf{W}, \tag{S22}$$

where the third equality uses the fact that $\mathbf{W}$ is the eigenvector matrix of $\mathbf{\Omega}$. Substituting $\mathbf{T} = \mathbf{W V}^{-1}$ into Eq. (S21) and then in Eq. (S20) yields the expressions in Eqs. (6) of the main text.

4. DERIVATIVE OF MATRIX EXPONENTIAL

Provided the matrix $\mathbf{\Omega}$ and its derivative $\mathbf{\Omega}'$ with respect to a design parameter, we compute the derivative of the matrix exponential $e^{j\mathbf{\Omega}L/k_0}$ through another the matrix exponential $e^{j\mathbf{G}L/k_0}$, where $\mathbf{G}$ is defined in Eq. (10) in the main text, and we repeat it here for convenience:

$$\mathbf{G} = \begin{bmatrix} \mathbf{\Omega} & \mathbf{\Omega}' \\ \mathbf{0} & \mathbf{\Omega} \end{bmatrix}.$$

To compute this matrix exponential efficiently (and avoid eigenvalue decomposition), we tailor the scaling and squaring method [3] to leverage the particular matrix structure of $\mathbf{G}$. We refer to [3] for the details of scaling and squaring method. To present how we tailor it for efficient computation, we outline its major steps here:

1. Compute an integer s to scale the matrix $j\mathbf{G}L/k_0$. Let $\tilde{\mathbf{G}}$ denote the scaled version: $\tilde{\mathbf{G}} = \frac{1}{2^s} j\mathbf{G}L/k_0$.
2. Compute two matrix polynomials, $D(\tilde{\mathbf{G}})$ and $N(\tilde{\mathbf{G}})$. The specific forms of these polynomials are determined by the scaling and squaring method.
3. Compute $\mathbf{A} = D^{-1}(\tilde{\mathbf{G}})N(\tilde{\mathbf{G}})$. The matrix inverse here is computed through matrix factorization.
4. Repeatedly square matrix $\mathbf{A}$ for s times, resulting in $\mathbf{B} = \mathbf{A}^{2^s}$. $\mathbf{B}$ is a close approximation of $e^{j\mathbf{G}L/k_0}$.

We notice that the matrix $\mathbf{G}$ has a specific structure—its lower-left block matrix is always a zero matrix, and its two diagonal block matrices are the same. This structure is preserved in $\tilde{\mathbf{G}}$ as well as in its matrix polynomials. We leverage this structure for accelerating the computation in two aspects.

First, in the computation of a matrix polynomial (step 2), we need to compute some matrix powers $\tilde{\mathbf{G}}^n$ for some integers n. Typically, $\tilde{\mathbf{G}}^n$ is expressed recursively as $\tilde{\mathbf{G}}\tilde{\mathbf{G}}^{n-1}$, and each recursion requires a multiplication of two $N \times N$ matrices, where N is the size of $\tilde{\mathbf{G}}$. In our computation, both $\tilde{\mathbf{G}}$ and $\tilde{\mathbf{G}}^{n-1}$ have the aforementioned block structure, and they can be represented as

$$\tilde{\mathbf{G}} = \begin{bmatrix} \mathbf{M}_1 & \mathbf{N}_1 \\ \mathbf{0} & \mathbf{M}_1 \end{bmatrix} \text{ and } \tilde{\mathbf{G}}^{n-1} = \begin{bmatrix} \mathbf{M}_2 & \mathbf{N}_2 \\ \mathbf{0} & \mathbf{M}_2 \end{bmatrix}. \tag{S23}$$

Their product is

$$\tilde{\mathbf{G}}\tilde{\mathbf{G}}^{n-1} = \begin{bmatrix} \mathbf{M}_1\mathbf{M}_2 & \mathbf{M}_1\mathbf{N}_2 + \mathbf{N}_1\mathbf{M}_2 \\ \mathbf{0} & \mathbf{M}_1\mathbf{M}_2 \end{bmatrix}, \tag{S24}$$

which involves three matrix multiplications of size $\frac{N}{2} \times \frac{N}{2}$. This is significantly faster than computing a multiplication of two $N \times N$ matrices.

Secondly, the two matrix polynomials $D(\tilde{\mathbf{G}})$ and $N(\tilde{\mathbf{G}})$ also have the same block structure, represented as

$$D(\tilde{\mathbf{G}}) = \begin{bmatrix} \mathbf{U}_1 & \mathbf{V}_1 \\ \mathbf{0} & \mathbf{U}_1 \end{bmatrix} \text{ and } N(\tilde{\mathbf{G}}) = \begin{bmatrix} \mathbf{U}_2 & \mathbf{V}_2 \\ \mathbf{0} & \mathbf{U}_2 \end{bmatrix}. \tag{S25}$$

Then, then the matrix product $D^{-1}(\tilde{\mathbf{G}})N(\tilde{\mathbf{G}})$ (in step 3) can be expressed as

$$D^{-1}(\tilde{\mathbf{G}})N(\tilde{\mathbf{G}}) = \begin{bmatrix} \mathbf{U}_1^{-1}\mathbf{U}_2 & \mathbf{U}_1^{-1}\mathbf{V}_2 - \left(\mathbf{U}_1^{-1}\mathbf{V}_1\right)\left(\mathbf{U}_1^{-1}\mathbf{U}_2\right) \\ \mathbf{0} & \mathbf{U}_1^{-1}\mathbf{U}_2 \end{bmatrix},$$

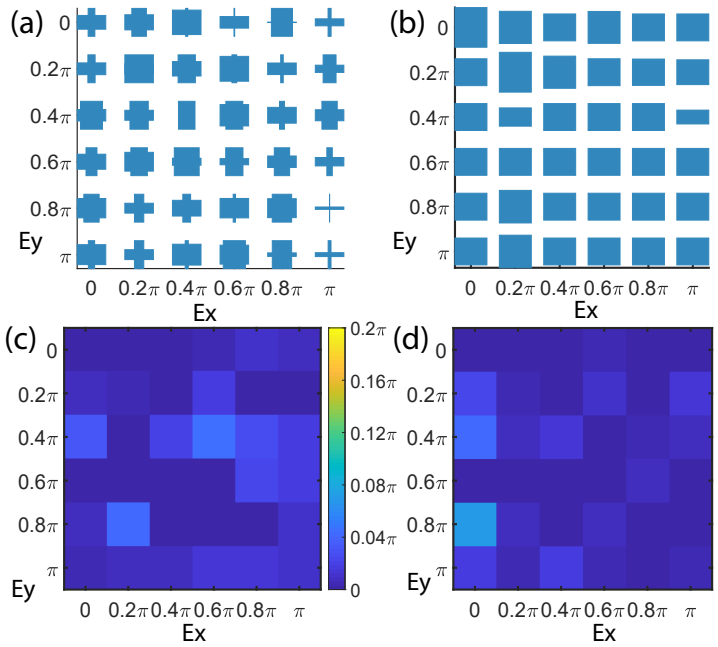

Fig. S1. Using meta-atom height as an additional parameter to control phrases. Here, we refine the meta-atom optimization reported in Fig. 6 by including another degree of freedom, the meta-atom's height. We start with the optimization results in Fig. 6, in which all meta-atoms have the same height. We then choose the 11 meta-atoms that have the largest optimization residual, and refine them by optimizing their in-plane parameters and their heights. (a) The cross-sectional shape designs of all meta-atoms after the refinement. (b) The resulting heights of the meta-atoms. (c) For x-polarized incident light, we show the phase difference between each pair of inversely designed phase change and the target. And similar visualization for y-polarized light is shown in (d). In comparison to Fig. 6-c and -d, the residuals are much smaller.

which involves only the matrix inverse (factorization) of the $\frac{N}{2} \times \frac{N}{2}$ matrix $\mathbf{U}_1$ and a few matrix multiplications of size $\frac{N}{2} \times \frac{N}{2}$. This is also much faster than computing $D^{-1}(\tilde{\mathbf{G}})N(\tilde{\mathbf{G}})$ directly.

5. META-ATOM HEIGHT AS ANOTHER OPTIMIZATION PARAMETER

While most of the current fabrication techniques require all meta-atoms on a metasurface to have the same height, advanced fabrication techniques (such as 3D printing) have no such a restriction, allowing each meta-atom to have its own height. The change of meta-atom's height does not alter the optical modes; it will only change the mode's propagation phase. As a result, only the matrix $\mathbf{X}$ in Eq. (4a) is affected, and its derivative with respect to the height L is constant, namely,

$$\mathrm{d}\mathbf{X} = j\frac{\Lambda}{k_0}\mathbf{X}. \tag{S26}$$

Nevertheless, we can include meta-atom's heights as another degree of freedom to further improve its performance. Here we revisit the numerical study that controls the phases for both x- and y-polarized light (reported in Fig. 6). Initially, all meta-atoms has the height $L = 2\mu m$. After our optimization in Fig. 6, we choose the meta-atoms that have relative large residuals (i.e., those corresponding to light-blue and green blocks in Fig. 6-c and -d). We then refine those meta-atoms by optimizing three parameters (two in-plane parameters as in Fig. 6 as well as the height L). As shown in Fig. S1, the performance of those meta-atoms are further improved.

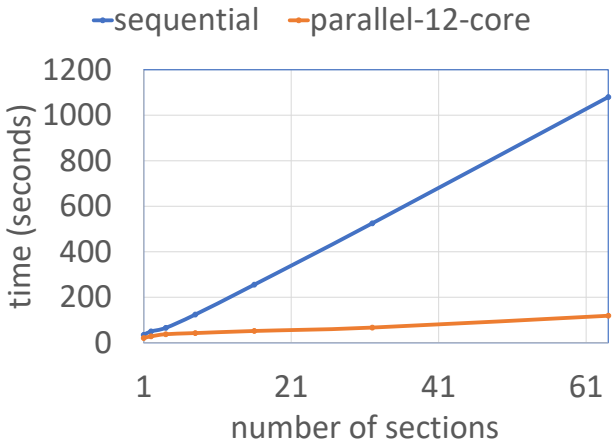

Fig. S2. Scalability. Here we use a simple photonic waveguide to examine the scalability of our method. The waveguide is made of silicon surrounded by SiO2. In our numerical analysis, the waveguide is split into N sections, each of which is described by 5 individual parameters. In total, the entire structure is specified by $5N$ parameters. If the scattering matrix derivative is computed using a straightforward sequential implementation, our method scales linearly as the number of section N increases (see blue curve). Here the y-axis indicates the time cost for computing all $5N$ derivatives on our workstation (whose hardware configuration is described in Section 4.1) When computed in parallel, our method scales sublinearly with respect to N.

6. SCALABILITY

An on-chip device such as the waveguide often has a cross-sectional shape varying along the propagation direction. To numerically analyze such a device, its structure is split into a series of sections, each of which is described by a scattering matrix, and the scattering matrix of the entire device can be computed using the Redheffer star product to combine the scattering matrices of all sections. Our method for computing the scattering matrix derivatives scales linearly with respect to the number of sections, as demonstrated in Fig. S2. Further, our proposed method can also be implemented as a parallel algorithm, as the scattering matrix of each section can be computed independently. If executed in parallel, our method has a much lower complexity, sublinear to the number of sections.

The source code of a C++ implementation of our proposed method can be downloaded from our GitHub repository.

REFERENCES

1. R. C. Rumpf, "Design and optimization of nano-optical elements by coupling fabrication to optical behavior," Ph.D. thesis, University of Central Florida (2006).
2. S.-W. Lee and R. Mittra, "Fourier transform of a polygonal shape function and its application in electromagnetics," IEEE Transactions on Antennas Propag. **31**, 99–103 (1983).
3. N. J. Higham, "The scaling and squaring method for the matrix exponential revisited," SIAM J. on Matrix Analysis Appl. **26**, 1179–1193 (2005).